

# Contact Changes near Jamming

Merlijn S. van Deen,<sup>1,\*</sup> Johannes Simon,<sup>1</sup> Zorana Zeravcic,<sup>2</sup> Simon Dagois-Bohy,<sup>1</sup> Brian P. Tighe,<sup>3</sup> and Martin van Hecke<sup>1,†</sup>

<sup>1</sup>*Huygens-Kamerlingh Onnes Lab, Universiteit Leiden, Postbus 9504, 2300 RA Leiden, The Netherlands*

<sup>2</sup>*School of Engineering and Applied Sciences, Harvard University, Cambridge, Massachusetts 02138, United States*

<sup>3</sup>*Process & Energy Laboratory, Delft University of Technology, Leeghwaterstraat 39, 2628 CB Delft, The Netherlands*

(Dated: April 21, 2022)

We probe the onset and effect of contact changes in soft harmonic particle packings which are sheared quasi-statically. We find that the first contact changes are the creation or breaking of contacts on a *single* particle. We characterize the critical strain, statistics of breaking versus making a contact, and ratio of shear modulus before and after such events, and explain their finite size scaling relations. For large systems at finite pressure, the critical strain vanishes but the ratio of shear modulus before and after a contact change approaches one: linear response remains relevant in large systems. For finite systems close to jamming the critical strain also vanishes, but here linear response already breaks down after a single contact change.

PACS numbers: 83.80.Fg, 83.10.Rs, 62.20.fg

Exciting progress in capturing the essence of the jamming transition in disordered media such as emulsions, granular matter, and foams has been made by considering the linear response of weakly compressed packings of repulsive, soft particles. When the confining pressure  $P$  approaches its critical value at zero, the resulting unjamming transition bears hallmarks of a critical phase transition: properties such as the contact number and elastic moduli exhibit power law scaling [1–7], time and length scales diverge [5, 8–10], the material’s response becomes singularly non-affine [10, 11] and finite size scaling governs the behavior for small numbers of particles  $N$  and/or small  $P$  [12–14].

However, such disordered solids are also extremely fragile near their critical points — even a tiny perturbation may lead to an intrinsically nonlinear response [15–21]. Hence, numerical studies of linear response have either resorted to simulations with very small deformations (strains of  $10^{-10}$  are not uncommon in such studies [22]), or have focussed on the *strict* linear response extracted from the Hessian matrix [10–12, 14].

Here we probe the first unambiguous deviations from strict linear response: contact changes under quasistatic shear (Fig. 1a). We focus on three questions: (i) What is the mean strain  $\gamma^c$  at which the first contact change arises?  $\gamma^c$  should vanish when either  $N$  diverges or  $P$  vanishes. We find a novel finite size scaling relation for  $\gamma^c$ , where  $\gamma^c \sim P$  for small systems close to jamming ( $N^2P \ll 1$ ), and  $\gamma^c \sim \sqrt{P}/N$  for  $N^2P \gg 1$ . (ii) What is the nature of the first contact changes? Plastic deformations under shear have been studied extensively in systems far from jamming, which display avalanches: collective, plastic events in which multiple contacts are broken and formed and the stresses exhibit discontinuous drops [23–27]. In contrast, we find that near jamming the first events are the making or breaking of a single contact, and that the stress remains continuous. The probabilities for contact making and breaking are governed by finite size scaling, with making and breaking equally likely for  $N^2P \gg 1$ , but contact breaking dominant for  $N^2P \ll 1$ . (iii) How do con-

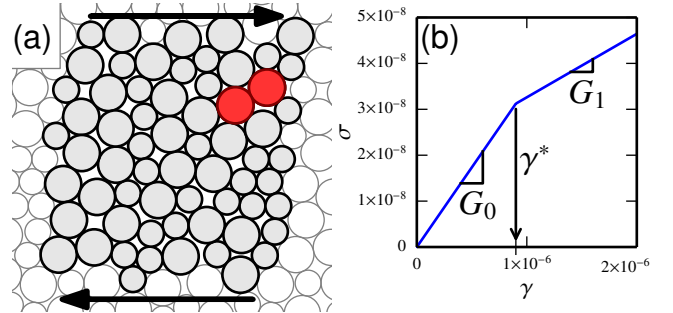


FIG. 1. (color online). (a) The first contact change in a sheared packing ( $N = 64$ ,  $P = 10^{-6}$ ) occurs at a strain  $\gamma^* = 9.003851(2) \times 10^{-7}$ , when the two marked particles lose their contact. (b) The corresponding stress-strain curve remains continuous but exhibits a sharp kink; we define  $G_0$  as the shear modulus of the undeformed packing, and  $G_1$  as the shear modulus of the packing just above  $\gamma^*$ .

tact changes affect linear response? For finite systems close to jamming, even a single contact change can strongly affect the elastic response (Fig. 1b). Clearly, calculations based on the Hessian matrix of the undeformed packing are then no longer strictly valid. As a result, the relevance of the linear response scaling relations are currently under dispute for systems close to jamming, at finite temperature, or in the thermodynamic limit [18, 28–32]. By comparing the shear modulus before ( $G_0$ ) and after ( $G_1$ ) the first contact change, we find that their ratio again is governed by finite size scaling, and while the ratio  $G_1/G_0$  approaches 0.2 for small  $N^2P$ , for large  $N^2P$ ,  $G_1/G_0 \rightarrow 1$ .

Our work suggests that while the range of *strict* validity of linear response vanishes for small  $P$  and large  $N$ , macroscopic quantities such as the shear modulus are relatively insensitive to contact changes as long as  $P \gg 1/N^2$ . Hence, linear response quantities remain relevant for finite  $P$  and large  $N$ , while for  $P \ll 1/N^2$ , a single contact change already changes the packing significantly. The qualitative differences in the nature of contact changes close to and far from jamming sug-

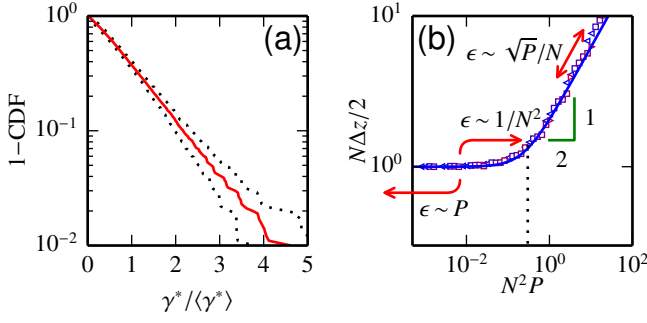


FIG. 2. (color online). (a) Complementary cumulative distribution function of  $\gamma^*/\langle\gamma^*\rangle$  (red line: median; black dotted lines: one  $\sigma$ ). (b) Scaling of  $N\Delta z/2$  as a function of  $N^2P$ . The arrows indicate volumetric strains corresponding to a single contact change.

gests that plasticity, creep, and flow *near* jamming are controlled by fundamentally different mechanisms than plastic flows in systems *far* from jamming [16, 17, 23, 25–27].

**Protocol:** We generate *shear stabilized* 2D packings of  $N$  soft harmonic particles with unit spring constant as described in [12]. Such shear stabilized packings are guaranteed to have a strictly positive shear modulus  $G_0$  and, moreover, have zero residual shear stress [12]. As  $\gamma^{cc}$  is expected to vanish for large  $N$ , finite size analysis is crucial, necessitating a wide range of system sizes — here  $N$  ranges from 16 to 4096 and we vary  $P$  from  $10^{-7}$  to  $10^{-2}$ .

To detect contact changes, we repeatedly impose small simple shear deformations  $\Delta\gamma$  at constant volume and let the system relax. When a change in the contact network is detected between strains  $\tilde{\gamma}$  and  $\tilde{\gamma} + \Delta\gamma$ , we determine the precise strain at the first contact change,  $\gamma^*$ , by bisection (i.e., going back to the system at  $\tilde{\gamma}$ , dividing  $\Delta\gamma$  by two, etc), resulting in an accuracy  $\Delta\gamma/\gamma^* < 10^{-6}$ .

The first contact changes come in different flavors, and we can distinguish isolated contact making or breaking, multiple contact making or multiple breaking events, and mixed events where contacts are both broken and created. In all these cases, rattlers need to be treated carefully. First, in approximately 1% of pure contact making events, a rattling particle becomes non-rattling, leading to the creation of three load bearing contacts. As these events depend on the ill-defined original location of the rattling particle, they are not included in the analysis. Secondly, a substantial fraction of contact breaking events (10-20%) leads to creation of rattlers, where not one but three contacts are broken simultaneously. This large proportion is not surprising, as weak contacts can easily be broken and are associated preferentially with near-rattling particles. These events, which are well-defined, are included in our statistics. Finally, mixed events start to play a role at high pressures, but even at  $P = 0.01$  less than 5% of the first events are composite, and their likelihood rapidly vanishes at lower pressures; Therefore we will not include these in our analysis. In the remainder of this Letter we focus on the statistics of the first contact making or breaking event.

**Characteristic Strain:** We find that for fixed  $P$  and  $N$ , the probability distribution of the strain  $\gamma^*$  at which the first contact making or breaking event arises closely resembles an exponential distribution. To show this, we have determined for all  $P$  and  $N$  the complementary cumulative distributions (which are also exponential), and in Fig. 2(a) we plot their median and indicate their 16th and 84th percentile. Their exponential nature implies that contact changes under shear can be seen as a Poisson process, and we define  $\gamma^{cc}$  as the ensemble average of  $\gamma^*$ . We note that while the underlying rate  $\sim 1/\gamma^{cc}$  is constant up to the first contact change, this rate can and will change beyond the first contact change.

As expected, we find that  $\gamma^{cc}$  increases with  $P$  and decreases for larger  $N$ . The question then arises: At what strain do we expect the first contact change? To start answering this, let us first consider changes in volume to derive a characteristic volumetric strain  $\epsilon^{cc}$  for the first contact change, in both small and thermodynamically large systems. We then demonstrate numerically that the same characteristic strain governs shear.

In Fig. 2(b) we sketch the scaling of the excess contact number  $\Delta z$  with pressure  $P$ , based on data reported in Refs. [12–14]. The scaling relation in the thermodynamic limit is well known,  $\Delta z \sim \sqrt{P}$  [2]. It is convenient to rewrite it in the extensive form  $N\Delta z \sim \sqrt{N^2P}$ . Making or breaking a contact increases or decreases  $N\Delta z/2$  by one, and the associated change in pressure  $\delta P$  can be determined from  $N\Delta z/2 \pm 1 \sim \sqrt{N^2(P \pm \delta P)}$ . The typical volumetric strain  $\epsilon^{cc} = \delta P/K \sim \delta P$  [33] so we obtain  $\epsilon^{cc} \sim \sqrt{P}/N$ .

The small system limit is different, as  $N\Delta z$  reaches a plateau independent of  $P$  and  $N$  — the system is one contact away from losing rigidity [12–14], as illustrated in Fig. 2(b). Hence contacts can only break when  $P \rightarrow 0$ , and the typical strain needed to break the last contact is  $\epsilon^{bk} \sim P$ . The strain to create an additional contact,  $\epsilon^{mk}$ , follows from the crossover between the two branches of  $N\Delta z$  in Fig. 2(b), so that  $\epsilon^{mk} \sim 1/N^2$ . The characteristic strain for the first contact *change*,  $\epsilon^{cc}$ , will be dominated by the smallest of the strains  $\epsilon^{mk}$  and  $\epsilon^{bk}$ . As for small systems  $N^2P \ll 1$ , it follows that  $\epsilon^{bk} \ll \epsilon^{mk}$ , so that contact breaking will dominate for small systems.

In summary, the characteristic strains under volumetric strain are predicted to be

$$\epsilon \sim \begin{cases} N^2P \ll 1: & \epsilon^{bk} = P & \epsilon^{mk} = 1/N^2 & \epsilon^{cc} = P, \\ N^2P \gg 1: & \sqrt{P}/N & \sqrt{P}/N & \sqrt{P}/N. \end{cases} \quad (1)$$

It follows that  $N^2\epsilon^{cc}$  will collapse when plotted as function of  $N^2P$ .

In Fig. 3(a) we plot our rescaled data for  $\gamma^{cc}$ , i.e. for *sheared* packings. Surprisingly, the scalings predicted for volumetric deformations *also* describe the characteristic strains for shear! Moreover, our collapsed data exhibits the two scaling regimes predicted in Eq. (1) for large and small values of  $PN^2$ .

We note that the data collapse of  $N^2\gamma^{cc}$  vs  $N^2P$  is good but not excellent. However, there is mounting evidence that the upper critical dimension of jamming is two, and several recent

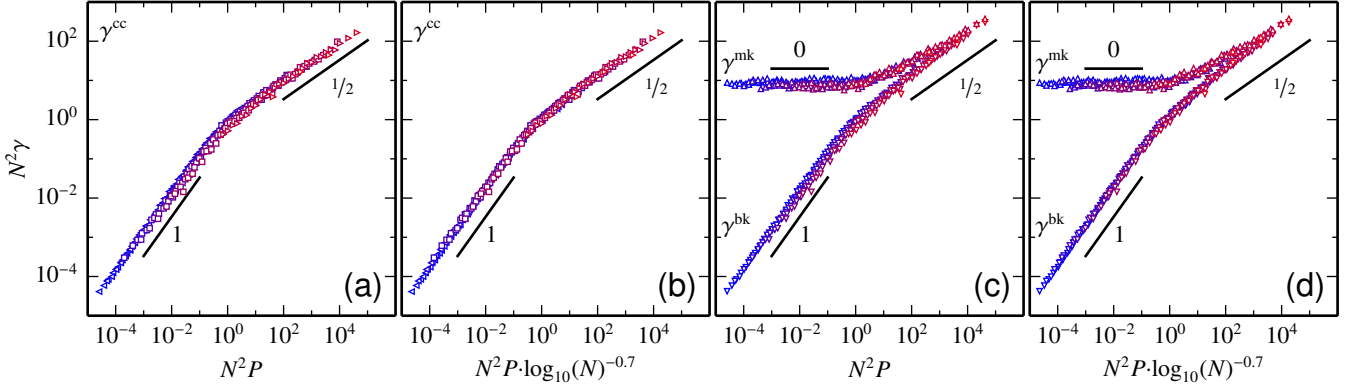


FIG. 3. (color online). Scaling of  $\gamma^{cc}$ ,  $\gamma^{bk}$  and  $\gamma^{mk}$ . (a) Scaling of the strain at first contact change. (b) Log corrections improve the collapse. In (a) and (b), symbols indicate packing sizes: ( $\circ$ ,  $N \leq 32$ ), ( $\square$ ,  $32 < N \leq 1024$ ) and ( $\triangleright$ ,  $N > 1024$ ). (c) Scaling of the strains for contact making ( $\Delta$ ) and contact breaking ( $\nabla$ ). (d) Again, log corrections improve the collapse.

accurate simulations of 2D systems near jamming show similar concomitant deviations from pure scaling [7, 14, 17, 34]. As recently determined for the scaling of the contact number in 2D, such corrections take the form of log corrections to  $N^2P$  of the form  $N^2P \log(N)^{-\beta}$ , with  $\beta \approx 0.7$  [14]. Inspired by this, we replot our data for  $\gamma^{cc}$  as a function of  $N^2P \log(N)^{-0.7}$ , and obtain very good data collapse (Fig. 3b). We conclude that the simple scaling arguments put forward in Eq. (1) capture the scaling of  $\gamma^{cc}$ .

*Making versus Breaking:* Our scaling argument makes separate predictions for the characteristic strains of the first creating and first destruction of contacts, but these are hard to determine independently in numerics. For example, for small  $N^2P$  we predict that  $\gamma^{mk} \gg \gamma^{bk}$ , but that means that almost all first contact change events are contact *breaking*, and even if we observe a few contact creations (in particular when breaking events occur at atypically large strains), there is a dependency between making and breaking events that cannot be disentangled in direct simulations.

To gain access to  $\gamma^{mk}$  and  $\gamma^{bk}$  independently, we use the fact that contact changes can be predicted from strict linear response. We start by extracting the linear prediction for the particle displacements  $\delta x_i$  under shear from the Hessian matrix as  $\Delta x_i = \gamma u_i$  [7, 10–12, 23, 27]. We then combine this with the overlaps and gaps between particles  $i$  and  $j$  at  $\gamma = 0$ , and determine the strain  $\gamma_{ij}$  at which contact  $ij$  is predicted to break or close. The minimum of  $\gamma_{ij}$  for all particle pairs in contact determines  $\gamma^{bk}$ , while the minimum for all pairs not in contact determines  $\gamma^{mk}$ . The minimum of both then determines  $\gamma^*$ .

The correspondence between the value of  $\gamma^*$  obtained from quasistatic simulations and  $\gamma^*$  obtained from linear response is excellent [35]. In the vast majority of cases we also identify the correct contact, and whether it breaks or is created; in the case of the creation of a rattler, linear response predicts a tightly bunched triplet of  $\gamma_{ij}$ 's.

Hence, strict linear response predicts its own demise. The

correspondence between quasistatic simulations and linear response also indicates that contact changes are the dominant source of nonlinearity (versus geometric effects). Using linear response we can thus calculate the strains where the first contact is created or broken and determine their mean values  $\gamma^{bk}$  and  $\gamma^{mk}$  as function of  $N$  and  $P$ .

In Fig. 3(c) we show the variation of  $N^2\gamma^{bk}$  and  $N^2\gamma^{mk}$  with  $N^2P$ , which confirms all the predicted scalings in Eq. (1): for large  $N^2P$ ,  $\gamma^{mk}$  approaches  $\gamma^{bk}$  and scales as  $\sqrt{P}/N$ , whereas for small  $N^2P$ ,  $\gamma^{mk}$  scales as  $1/N^2$ , whereas  $\gamma^{bk} \sim P$ . As before, the data collapse is reasonably good, and gets improved by the aforementioned log-corrections (Fig. 3(d)).

*Effect of a single contact change:* What happens for strains larger than  $\gamma^*$ ? It has been suggested that, for purely repulsive particles, linear response is no longer valid for large  $N$  [18], leading to a lively debate [28, 29, 32]. On the one hand, it is clear that for small systems, the breaking or creation of a single contact can have a substantial effect, in particular close to jamming (see Fig. 1(b)) — but what happens for larger systems? Our data implies that  $\gamma^*$  vanishes in the thermodynamic limit, so the question is what, then, is the relevance of linear response quantities?

To probe the relevance of linear response, we determined the distribution  $P(G_1/G_0)$ , where  $G_0$  and  $G_1$  denote the shear modulus before and after the first contact change (Fig. 4). We find that the shape of these distributions varies widely and is determined by  $N^2P$ . We can distinguish three regimes: (i) For  $N^2P \ll 1$ ,  $G_1 < G_0$  and  $\langle G_1/G_0 \rangle \approx 0.2$ . The signs of  $G_0$  and  $G_1$  are both positive in this regime.  $G_0$  has to be positive as we use SS packings [12]. The sign of  $G_1$  is not immediately obvious, but we note that for it to become negative, a finite prestress is needed, but for  $P \rightarrow 0$  this prestress vanishes so that  $G_1$  remains positive here [14]. (ii) For  $N^2P \approx 1$ , the prestresses become important, but as the number of excess contacts is still small,  $G_1$  now can become negative. Indeed we find that  $P(G_1/G_0)$  has a wide distribution which now acquires a finite weight for negative  $G_1/G_0$ .

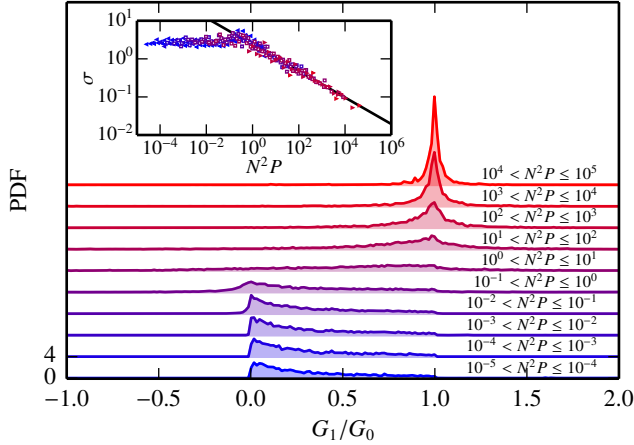


FIG. 4. (color online). The probability distribution functions of  $G_1/G_0$  for a range of values of  $N$  and  $P$  become narrowly peaked when  $N^2P$  becomes large. We offset curves for different  $N^2P$  for clarity. Inset: the standard deviation  $\sigma$  of the distribution of  $G_1/G_0$  vanishes as  $(N^2P)^{-\beta}$ , with  $\beta = 0.35 \pm 0.01$ , as indicated by the fitted line.

(iii) For  $N^2P \gg 1$ ,  $G_1$  approaches  $G_0$ , and the distribution  $P(G_1/G_0)$  becomes sharper with increasing  $N^2P$ . This can be understood by noting that for  $N^2P \gg 1$ , making and breaking of contacts is equally likely, and that  $G$  varies as  $\Delta z$ . As the width of  $P(G_1/G_0)$  scales as the difference in  $G_1/G_0$  when either a contact is added or removed, we estimate the values of  $G_1$  as  $G^+ \sim \Delta z_0 + 1/N$  and  $G^- \sim \Delta z_0 - 1/N$ , and thus  $(G^+ - G^-)/G_0 \sim (1/N)/\Delta z_0 \sim 1/\sqrt{N^2P}$ .

As shown in Fig. 4, the standard deviation of  $P(G_1/G_0)$  vanishes for large  $N^2P$  as  $(N^2P)^{-\beta}$  with  $\beta \approx 0.35$ , i.e. somewhat slower than predicted. As we will argue now, as long as  $\beta > 1/4$ ,  $G$  is still well defined in the thermodynamic limit.

Let us ask the following: Can we estimate the deviation in  $G$  in the thermodynamic limit for a fixed strain  $\gamma_i$ ? For large  $N^2P$ , making and breaking events are equally likely, and as  $\gamma^c \sim \sqrt{P}/N$ , the number of these events for fixed strain  $\gamma_i$  can be estimated to diverge as  $N/\sqrt{P}$ . Under the assumption that each of these events are drawn independently from a distribution with a variance that scales as  $(N^2P)^{-2\beta}$ , we find that the variance in  $G_1$  is of order  $N^{1-4\beta}P^{-1/2-2\beta}$ , which converges to zero in the large  $N$  limit when  $\beta > 1/4$ , as is clearly the case here. We believe this to be consistent with a picture where, for large systems, the effective value of  $G$  depends on the strain only, and not on the total number of contact changes [34, 36].

*Discussion:* We now compare our work to recent studies of contact changes in nonlinearly vibrated jammed packings [18]. Consistent with our work, contact changes occur for vanishingly small perturbations when either  $N \rightarrow \infty$ , or  $P \rightarrow 0$ . Nevertheless, the obtained scaling relations are different. We note that the procedure used in [18] is very different: Schreck *et al* vibrate their packings and select the critical

perturbation amplitude by minimizing over all eigenmodes, whereas our protocol employs a single mode of deformation.

We clarify here that even though the first contact change signals the end of *strict* linear response, its predictions for macroscopic observables such as the shear modulus remain relevant far beyond the first contact change. A wider implication of our work is to uncover the unique character of rearrangements in marginal materials: Microscopic rearrangements in systems in the vicinity of a jamming transition are restricted to the particle scale, which is qualitatively distinct from denser amorphous systems, which are dominated by collective, avalanche-like events.

We thank L Gomez, S Henkes, CP Goodrich, AJ Liu, SR Nagel and CS O'Hern for discussions. SDB acknowledges funding from the Dutch physics foundation FOM, and MvD, BPT and MvH acknowledge funding from the Netherlands Organization for Scientific Research (NWO).

\* [deen@physics.leidenuniv.nl](mailto:deen@physics.leidenuniv.nl)

† [hecke@physics.leidenuniv.nl](mailto:hecke@physics.leidenuniv.nl)

- [1] F. Bolton and D. Weaire, *Phys. Rev. Lett.* **65**, 3449 (1990).
- [2] D. J. Durian, *Phys. Rev. Lett.* **75**, 4780 (1995).
- [3] M.-D. Lacasse, G. S. Grest, D. Levine, T. G. Mason, and D. A. Weitz, *Phys. Rev. Lett.* **76**, 3448 (1996).
- [4] C. S. O'Hern, S. A. Langer, A. J. Liu, and S. R. Nagel, *Phys. Rev. Lett.* **88**, 075507 (2002).
- [5] C. S. O'Hern, L. E. Silbert, A. J. Liu, and S. R. Nagel, *Phys. Rev. E* **68**, 011306 (2003).
- [6] G. Katgert and M. van Hecke, *Europhys. Lett.* **92**, 34002 (2010).
- [7] B. P. Tighe, *Phys. Rev. Lett.* **107**, 158303 (2011).
- [8] M. Wyart, S. R. Nagel, and T. A. Witten, *Europhys. Lett.* **72**, 486 (2005).
- [9] L. E. Silbert, A. J. Liu, and S. R. Nagel, *Phys. Rev. Lett.* **95**, 098301 (2005).
- [10] W. G. Ellenbroek, E. Somfai, M. van Hecke, and W. van Saarloos, *Phys. Rev. Lett.* **97**, 258001 (2006).
- [11] W. G. Ellenbroek, M. van Hecke, and W. van Saarloos, *Phys. Rev. E* **80**, 061307 (2009).
- [12] S. Dagois-Bohy, B. P. Tighe, J. Simon, S. Henkes, and M. van Hecke, *Phys. Rev. Lett.* **109**, 095703 (2012).
- [13] C. P. Goodrich, A. J. Liu, and S. R. Nagel, *Phys. Rev. Lett.* **109**, 095704 (2012).
- [14] C. P. Goodrich, S. Dagois-Bohy, B. P. Tighe, M. van Hecke, A. J. Liu, and S. R. Nagel, in prep.
- [15] M. Wyart, *Phys. Rev. Lett.* **109**, 125502 (2012).
- [16] P. Olsson and S. Teitel, *Phys. Rev. Lett.* **99**, 178001 (2007).
- [17] B. P. Tighe, E. Woldhuis, J. J. C. Remmers, W. van Saarloos, and M. van Hecke, *Phys. Rev. Lett.* **105**, 088303 (2010).
- [18] C. F. Schreck, T. Bertrand, C. S. O'Hern, and M. D. Shattuck, *Phys. Rev. Lett.* **107**, 078301 (2011).
- [19] L. R. Gómez, A. M. Turner, and V. Vitelli, *Phys. Rev. E* **86**, 041302 (2012).
- [20] L. R. Gómez, A. M. Turner, M. van Hecke, and V. Vitelli, *Phys. Rev. Lett.* **108**, 058001 (2012).
- [21] S. van den Wildenberg, R. van Loo, and M. van Hecke, *Phys. Rev. Lett.* **111**, 218003 (2013).
- [22] C. F. Schreck and C. S. O'Hern, *Experimental and computa-*

*tional techniques in soft condensed matter physics* (Cambridge Univ. Press, 2010).

- [23] C. E. Maloney and A. Lemaître, [Phys. Rev. E \*\*74\*\*, 016118 \(2006\)](#).
- [24] A. Lemaître and C. Caroli, [Phys. Rev. E \*\*76\*\*, 036104 \(2007\)](#).
- [25] K. M. Salerno, C. E. Maloney, and M. O. Robbins, [Phys. Rev. Lett. \*\*109\*\*, 105703 \(2012\)](#).
- [26] H. G. E. Hentschel, S. Karmakar, E. Lerner, and I. Procaccia, [Phys. Rev. Lett. \*\*104\*\*, 025501 \(2010\)](#).
- [27] M. L. Manning and A. J. Liu, [Phys. Rev. Lett. \*\*107\*\*, 108302 \(2011\)](#).
- [28] C. P. Goodrich, A. J. Liu, and S. R. Nagel, [Phys. Rev. Lett. \*\*112\*\*, 049801 \(2014\)](#).
- [29] C. F. Schreck, T. Bertrand, C. S. O'Hern, and M. D. Shattuck, [arXiv:1306.1961](#).
- [30] A. Ikeda, L. Berthier, and G. Biroli, [J. Chem. Phys. \*\*138\*\*, 12A507 \(2013\)](#).
- [31] L. Wang and N. Xu, [Soft Matter \*\*9\*\*, 2475 \(2013\)](#).
- [32] C. P. Goodrich, A. J. Liu, and S. R. Nagel, [arXiv:1402.6206](#).
- [33] The bulk modulus  $K$  is  $O(1)$  in packings of soft harmonic spheres [5].
- [34] S. Dagois-Bohy, E. Somfai, B. P. Tighe, and M. van Hecke, in prep.
- [35] See Supplemental Material at [URL will be inserted by publisher] for probability distribution functions of  $\gamma_{LR}^*/\gamma_{MD}^*$  for different packing sizes.
- [36] J. Boschan, E. Somfai, and B. P. Tighe, in prep.

*Supplementary material*

We have studied the correspondence between the characteristic strains in strict linear response,  $\gamma_{\text{LR}}$ , and from quasistatic shear simulations,  $\gamma_{\text{QS}}$ . The largest deviations are found for small systems and large pressures, as here the characteristic strain is largest. In Fig. 5 we show probability distributions of the ratio  $\gamma_{\text{LR}}/\gamma_{\text{QS}}$ , which illustrate this.

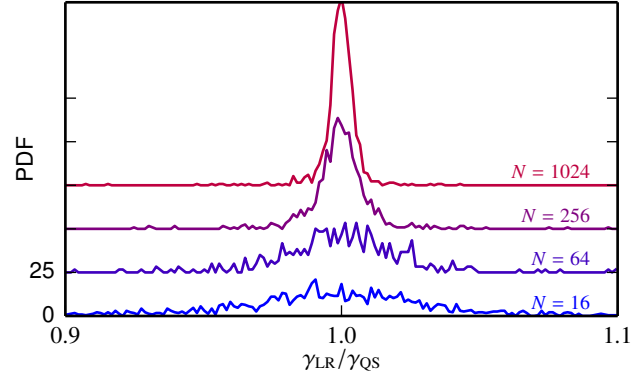


FIG. 5. Distribution of  $\gamma_{\text{LR}}/\gamma_{\text{QS}}$  for different packing sizes at  $P = 10^{-2}$  (worst case scenario). Curves have been offset for clarity. The largest deviations are seen for  $N = 16$ , but even there deviations are smaller than 10%.